INDUSTRIAL PROCESS STEAM GENERATION FROM DEEP GEOTHERMAL RESERVOIRS

Sven Klute[1]*, Mathias van Beek[1], Marcus Budt[1]

[1] Fraunhofer Institute for Environmental, Safety, and Energy Technology UMSICHT, 46047 Oberhausen, Germany

*Corresponding Author: sven.klute@umsicht.fraunhofer.de

ABSTRACT

Deep geothermal reservoirs (depth > 400 m) have been used to provide heat and electricity for decades. Heating of industrial processes, however, is one of the less common applications and accounts for under 1 % of the total installed capacity. One of the main reasons for this low share is the temperature level of geothermal sources, which is often unsuitable for direct heating of industrial processes. In addition, process steam is commonly used as heat transfer medium in industry, making the integration of geothermal energy even more challenging. This paper presents technical solutions to overcome these restrictions. In a first step, state-of-the-art systems are presented. These systems are limited to generating process steam at a temperature level below that of the geothermal source. Subsequently, R&D approaches from the literature are presented which aim to provide higher temperatures through additional energetic upgrading. Based on these findings, three promising concepts with steam generating heat pumps (SGHP) are presented and examined in a simulative case study. The first concept is using a closed-loop compression heat pump (CLCHP) with direct steam generation in the heat pump condenser. The second concept consists of a combination of CLCHP with direct steam generation and a downstream mechanical vapor recompression (MVR) unit. In the third concept, an evaporator and an MVR are used. In the case study, two geothermal sources with a temperature of 100 °C (50 l/s) and 80 °C (50 l/s) are considered and cooled down to up to 60 °C. On the sink side, superheated steam with 150 °C and 4 bar is generated from a water source with 20 °C and 1 bar. A sensitivity analysis is conducted to investigate the effects of the isentropic compressor efficiency (MVR) and the efficiency of the CLCHP. An extended coefficient of performance COP_{PR} is used for the evaluation, which, in addition to the electrical demand of the heat pump, also includes the required pumping effort for the geothermal fluid. For the investigated cases, the third process route achieves the highest COP_{PR} of 4.25, when cooling the geothermal source from 100 °C to about 84 °C and 3.4 when cooling the geothermal source from 80 °C to about 64 °C. A comparison with alternative steam generation technologies (gas boilers, electric boilers and green hydrogen boilers) also highlights the ecological advantages (CO_2-Emissions and primary energy demand) of geothermal steam generation.

Keywords: renewable energy, process steam, high-temperature heat pumps, steam generating heat pumps, geothermal energy

1 INTRODUCTION

Process heat is one of the most important energy demands in the industrial sector. In Germany, for example, almost 67 % of final industrial energy consumption is used to provide industrial process heat (BMWK, 2022a). Due to technical and economic constraints, less than 6 % of this heat is currently covered by renewable energies (BMWK, 2022b). In addition, many sectors use process steam as a heat transfer medium, which makes the integration of renewable energies difficult. In the current debate, green hydrogen is often cited as the key technology for solving this problem. However, there are more efficient and resource-saving alternatives, especially for the temperature range up to 500 °C (Agora Industrie, 2022). Besides direct electrification, the integration of renewable heat sources such as deep geothermal energy can be particularly advantageous. With its base load capability, deep geothermal

https://doi.org/10.52202/077185-0028

energy offers great potential for meeting this demand. However, as the temperature level of the geothermal source is generally too low to provide steam directly at the required temperature and pressure level, thermal upgrading is required.
In the past, thermal upgrading was avoided due to the increased cost and technical limitations. Instead, suitable heat consumers that can be served directly by the geothermal source were addressed (Lassacher *et al.*, 2018). As a result, the current state of knowledge in this area – particularly in the case of steam generation – is limited (Chapter 2). However, this application is becoming increasingly interesting due to the ambitious climate policy targets and technical developments in the field of thermal upgrading. Thermal upgrading in combination with steam generation offers great potential. In Germany alone, supplying process heat up to 300 °C could cover around 90 TWh/a (Schmitt, 2014).
For the supply of process steam, steam-generating heat pumps (SGHP) are particularly suitable. With current technologies, temperatures of up to 350 °C can be achieved (Klute *et al.*, 2024). Due to the technological diversity, there are numerous configurations, which are described in more detail in (Klute, 2024; Klute *et al.*, 2024). In Chapter 3, three promising configurations are presented and investigated in a sensitivity analysis in Chapter 4.

2 Direct utilization of geothermal energy

Direct utilization of geothermal energy (without electricity generation) is one of the oldest forms of geothermal energy utilization and has been present for over 2,000 years (Lund and Toth, 2020). The numerous applications can be grouped into different categories according to Table 1. The most common applications are geothermal heat pumps with near-surface sources, space heating (including district heating) as well as hot water supply for bathing and swimming.
With an installed capacity of 852 MW, industrial use accounts for only 0.7 % of total global geothermal capacity. The plants are operated in 14 different countries and are usually designed with large capacities and high operating hours (Lund and Toth, 2020). An additional plant is currently being planned in Croatia (Vasiljević, 2019). In the first stage of the project, geothermal water at 150–200 °C is to be used to heat process water and buildings. In a second phase, the plant is subsequently expanded to include electricity generation as well.

Table 1: Installed capacity of geothermal power generation and direct utilization in 2020 (HUTTRER, 2020; Lund and Toth, 2020)

Utilization	Capacity [MW]	Share [%]
Total	123,677	100
Power Generation	15,950	12.9
Direct Utilization (sum)	107,727	87.1
Geothermal heat pumps (ground-source)	77,547	62.7
Space heating	12,768	10.3
Bathing and swimming	12,253	9.9
Greenhouse heating	2,459	2.0
Aquacultural pond heating	950	0.8
Industrial use	852	0.7
Other	798	0.7

Due to the limited number of projects, there is a lack of experience with supplying industrial heat. This leads to skepticism among many potential users. However, the exploration of suitable sources is well known from other types of applications such as district heating. Hydrothermal doublets have become a standard system for providing deep geothermal energy. A hydraulically conductive underground formation is tapped via a production and injection well. The naturally occurring geothermal water is heated by the surrounding rock formations and pumped to the surface for thermal utilization. After heat extraction, the cooled geothermal water is then fed back into the underground, where it heats up once again. (Bracke and Huenges, 2021)
Figure 1 shows a typical setup for direct use applications. In most systems, a closed-loop geothermal water system is used to prevent the migration of unwanted components of the geothermal water such as

https://doi.org/10.52202/077185-0028

dissolved gases into the process media (Lund, 2010). Open-loop systems are an exception and are only used if the chemical composition of the geothermal water is irrelevant for the process (Sigurdsson, 1992) or if it can be adapted with additional technical effort (Carter and Hotson, 1992).
Electrical submersible pumps or line shaft pumps are usually installed into the production well to extract the geothermal water (Brasser *et al.*, 2014). In order to compensate systemic pressure fluctuations, the systems are equipped with pressure equalization tanks which are filled with a mixture of geothermal water and inert gases (gec-co, 2019). The operating pressure of the system is usually up to 16 bar or even above (Kaltschmitt, 2013). Before entering the heat exchangers, the geothermal water is cleaned of larger particles using coarse filters (e. g. backwash, basket and bag filters) (gec-co, 2019). For the heat extraction, shell-and-tube heat exchangers or bolted or welded plate heat exchangers are used (Kaltschmitt, 2013; gec-co, 2019). The heat exchanger material is selected according to the geothermal water composition. For highly corrosive media, titanium is mainly used (Kaltschmitt, 2013). If the system pressure is not sufficient to overcome the pressure losses in the injection borehole, additional injection pumps must be installed. As these pumps can be installed above the surface, no special pump designs are required (Brasser *et al.*, 2014). As a result of the temperature reduction, precipitation, scaling and changes in chemical properties (e. g. pH value) of the geothermal water can occur. To prevent damage to the injection well, fine filters are therefore used before injection (Kaltschmitt, 2013).

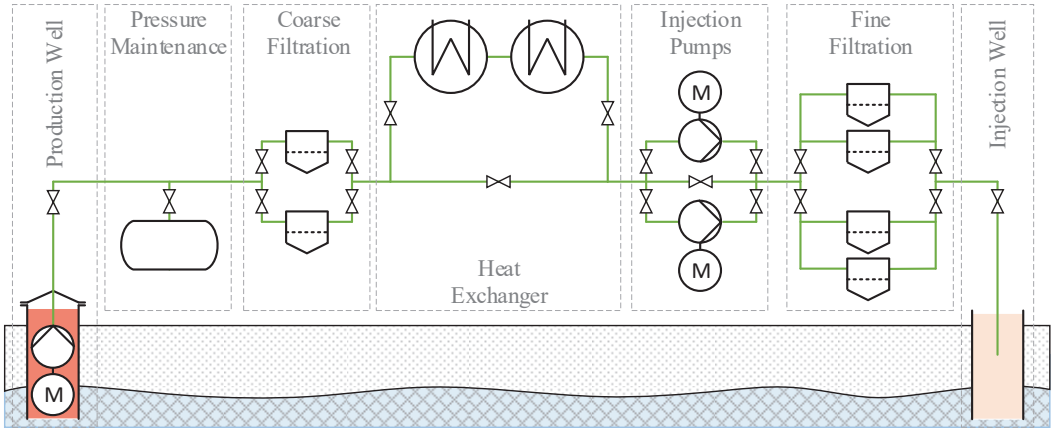

Figure 1: Typical layout of a geothermal plant for heat generation according to (Kaltschmitt, 2013)

Deep geothermal systems as shown in Figure 1 have so far been used almost exclusively for applications with heat demand at a temperature level below the reservoir temperature (Lassacher *et al.*, 2018). However, if the temperature and/or heat capacity is insufficient, additional units such as peak load boilers or heat pumps can be installed (Kaltschmitt, 2013). For example, Stadtwerke Schwerin is currently planning a heat pump system to heat up the geothermal water (depth 1,300 m) from 56 °C to 80 °C and feed it into a district heating network (Stadtwerke Schwerin). Steam generation from deep geothermal reservoirs is significantly less developed in comparison and will be described in more detail in the following sections.

2.1 Geothermal steam generation – state of the art

To date, geothermal steam generation has only been used in combination with wet and dry steam reservoirs (Zarrouk and Purnanto, 2015). Due to high reservoir temperatures of over 180 °C, the geothermal water is provided as dry steam or a two-phase mixture and can be used for power generation in dry steam plants or flash-plants (Lund, 1997; Kaltschmitt, 2013). In some applications, the geothermal steam is directly used as working fluid of the power plant. In general, however, steam from geothermal sources is strongly mineralized (e. g. with sulphur or boron) so that direct use in a turbine or process is often not possible. In these cases, secondary loops with heat exchangers are applied (Lund, 2010; Pelte, 2010).
Besides power generation, only one application is currently known for using geothermal steam in an industrial process. The plant at the Kawerau site in New Zealand has been in operation since the 1950s

https://doi.org/10.52202/077185-0028

and supplies steam for pulp and paper production. Figure 2 shows a simplified process layout of the steam generating plant. The geothermal water is extracted at around 270 °C and gets separated into a vapor and liquid phase through a flash system. Due to unwanted components – such as non-condensable gases, which can accumulate in the components and impair heat transfer or pose an increased safety risk in the event of leaks – the vapor phase is unsuitable for direct use in the paper mill processes. Instead, the vapor phase is fed into heat exchangers (steam converter) and used to evaporate treated feedwater. The described plant was designed to provide process steam at 3.45 and 10.45 bar using a vapor phase at 7 and 14 bar. The condensate return is used as feedwater for the process steam. In the first years of operation, it was not possible to guarantee sufficient feed water quality, which led to corrosion and fouling problems in the steam converter. These problems were solved after implementing a multi-stage water treatment system. (Carter and Hotson, 1992; Bloomer, 2011)

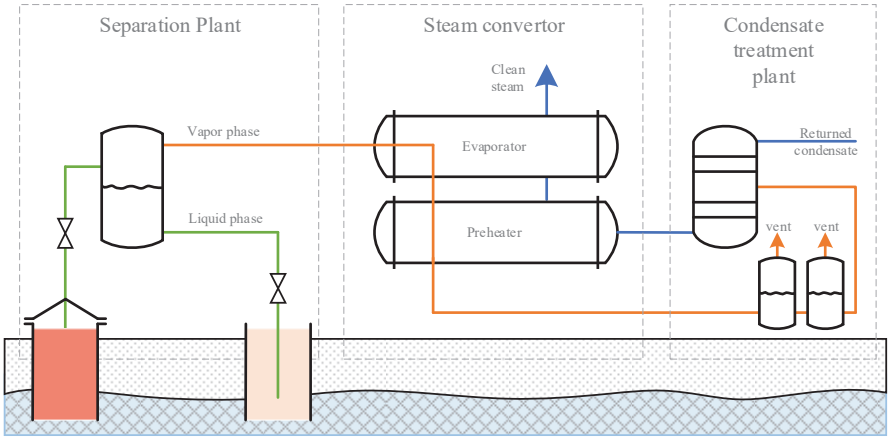

Figure 2: Simplified plant layout for geothermal steam generation at Kawerau, New Zealand according to (Carter and Hotson, 1992)

2.2 Geothermal steam generation – R&D

For sites with moderate reservoir temperatures, the process described in Section 2.1 is only applicable to a limited extent, as the required process steam temperatures are often higher than the existing reservoir temperature. In such cases, steam generation can only be carried out in combination with thermal upgrading. Such a setup has not yet been implemented at any site. Furthermore, only a few theoretical approaches have been published in the literature which are clustered into six basic concepts in Figure 3. The configurations A to C are designed for direct use of geothermal steam, which makes them less suitable for industrial use. In the configurations D to F, a secondary circuit with clean feed water is used to avoid potential problems caused by the geothermal water.

In configuration A, geothermal water is firstly flashed to generate a vapor phase, which is then heated up by fossil fuel combustion. Due to the flash process, the maximum steam pressure is limited by the reservoir temperature. The subsequent fossil heating only allows the saturated steam to be superheated. If the fossil fuel combustion is arranged upstream of the flash tank (configuration B), maximum achievable steam pressure can be increased instead. In this configuration, however, only saturated steam can be produced. (Lienau and Lunis, 1991)

Configuration C combines a flash tank with subsequent mechanical vapor compression (MVR) (Lienau and Lunis, 1991). The authors suggest a binary cycle with isobutane (organic rankine cycle) to provide the motive power for the compressor. The liquid phase from the flash tank is used as a heat source. The process route was investigated theoretically for reservoir temperatures in the range of 121–176 °C. The compressed steam can be discharged at different temperature levels (e. g. 118 °C, 160 °C or 182 °C). As an alternative, electric motors can be used to drive the compressors. A similar setup was investigated for reservoir temperatures of 50–150 °C (Ungar *et al.*, 2023). The hot geothermal water is first partially evaporated in a flash tank and then compressed in multiple stages. The superheated steam is passed through heat exchangers for intercooling and additional heating of the flash tank. The system is intended

https://doi.org/10.52202/077185-0028

to provide steam at 10–15 bar (180–200 °C saturated steam temperature). In a simulative case study, a COP (coefficient of performance) in the range 1–5 was calculated.
Configuration D contains a CLCHP with direct steam generation. Geothermal water is used as heat source, while the feedwater serves as heat sink. In the research project STEPs, a demonstrator with a two-stage compression heat pump was build and tested with freshwater (52–97 °C) instead of thermal mater. The target steam temperature was in the range of 120–150 °C. On a laboratory scale (150 kW_{th}), it was possible to generate process steam at 150 °C from source temperatures of 65 °C with a COP of 2.1 (Spoelstra, 2019). A comparable setup with geothermal water temperatures in the range of 50 to 150 °C was investigated in a simulative study (Ungar *et al.*, 2023). The saturated steam (180–200 °C) is directly evaporated in the heat pump condenser (shell-and-tube design).
Configuration E consists of a CLCHP with a downstream flash tank. The heat pump heats pressurized feed water to up to 130 °C. The hot water is then partially expanded in a flash tank to provide saturated steam at about 100 °C. As a heat source, geothermal water with 50–70 °C was considered. The theoretical study focused on the selection of suitable refrigerants. A maximum COP of 3.8 was reached when using R141b as working fluid. (Lu *et al.*, 2019)
The configuration F combines a flash tank with a steam converter and a downstream mechanical vapor compression. The geothermal water is firstly separated into a vapor and liquid phase (flash process). The saturated steam is then condensed in a steam converter to evaporate feed water. As the generated process steam does not yet meet the required process steam parameters, additional vapor compression with MVR is used. The case study investigated an application with geothermal water at 170 °C and 8 bar for the supply of process steam at 184 °C and 10.5 bar. (Walmsley *et al.*, 2016)

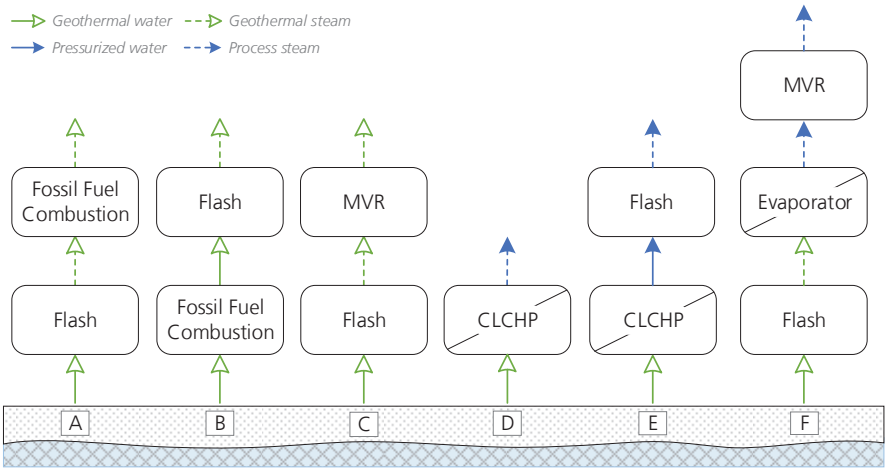

Figure 3: R&D systems for geothermal steam generating with thermal upgrading according to (Klute, 2024). MVR = Mechanical vapor recompression, CLCHP = Closed-loop compression heat pump

Despite the limited scope of research to date, geothermal steam generation offers great potential for the future. Numerous SGHPs already exist today, which can be adapted for use with geothermal sources (Klute *et al.*, 2024). One major challenge is the technological diversity, which leads to a large number of potential system configurations. In (Klute, 2024), a methodology has therefore been developed with which suitable process routes can be identified for specific applications. In the following chapter, three promising process routes are presented and compared with alternative steam generation systems.

3 Case study

In this case study, three exemplary process routes (PR) for steam generation from two different geothermal sources are investigated (Figure 4). The first source (G1) has a reservoir temperature of 100 °C and a flow rate of 50 l/s. The second source (G2) is slightly colder with 80 °C and a flow rate of 50 l/s. In both cases, a production pump (depth 250 m) is required to tap the reservoir and to maintain the system pressure of the geothermal loop (15 bar). No additional injection pump is required.

https://doi.org/10.52202/077185-0028

The generated steam is produced from feedwater at 20 °C and 1 bar and fed into an industrial steam network at a pressure of 4 bar and 150 °C (6.4 K superheated). To prevent the geothermal water from entering the process or the product, a secondary loop with pressurized water (2 bar) is installed in all PR.

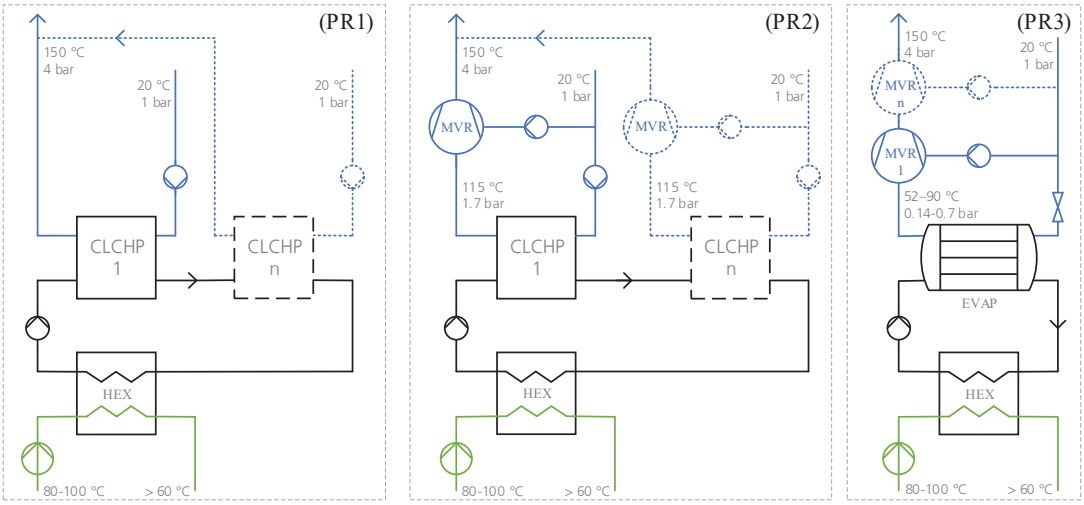

Figure 4: Flowsheets of the three investigated process routes. CLCHP = Closed-loop compression heat pump, HEX = Heat exchanger, EVAP = Evaporator, MVR = Mechanical vapor recompression

PR1 is equipped with a CLCHP, which uses the water of the secondary loop as heat source. The feedwater is directly evaporated and superheated in the condenser of the heat pump loop. The maximum temperature glide at the heat source is typically limited to a maximum value of 20 K per heat pump unit (Klute *et al.*, 2024). Higher glides can be achieved by serially connecting several heat pump units. For this study, it is assumed that all units provide the same target temperature. This results in a higher temperature lift and therefore a lower COP for downstream heat pump units.

PR2 is equipped with a CLCHP and an MVR. The CLCHP generates saturated steam at 1.7 bar (115 °C), which is then further compressed by MVR. The intermediate pressure level was selected to ensure a single-stage MVR compression at all operating points but can be varied for optimization purposes. Each MVR stage is equipped with water injection for temperature control. A serial connection is used for large temperature glides above 20 K.

PR3 consists of an evaporator with downstream MVR. The evaporation pressure can be adjusted to influence the injection temperature of the geothermal water. In general, a reduction in the evaporation pressure leads to a reduction in the injection temperature. As the evaporation pressure decreases, however, the pressure ratio of the MVR increases. If the design-dependent maximum value is reached, it is therefore necessary to switch to a serial configuration with multiple MVR units. In this study, a maximum pressure ratio of 2.5 is chosen (Klute *et al.*, 2024). In case of multi-stage compression, it is assumed that the previous compressor stage always applies the maximum pressure ratio. The compressed steam is cooled to saturated steam conditions between each compressor stage.

As a comparison, three alternative systems for steam generation are considered. Technology 1 (T1) is a conventional steam boiler with economizer (natural gas, boiler efficiency 95 % (Bosch, 2023)), Technology 2 (T2) is a hydrogen boiler (green hydrogen, boiler efficiency 90 % (TNO, 2020)) and Technology 3 (T3) is an electric steam boiler (boiler efficiency 99 % (Agora Industrie *et al.*, 2022)).

3.1 Simulation Models

Simulation models were implemented in Dymola (v. 2023x), which uses the object-oriented programming language Modelica (v. 4.0). The models are based on the open-source library ClaRa (v. 1.5.1) and got adapted to meet the requirements of this study. The relevant assumptions of these models are explained below. More detailed information on this can be found in (Klute, 2024).

The electrical power consumption of the production pump $P_{el,P}$ is calculated assuming an incompressible medium in accordance with Equation (1). The delivery head H is set at a constant value

https://doi.org/10.52202/077185-0028

of 250 m. The density ρ and the volume flow rate $\dot{V}$ represent the values of the geothermal water at the pump inlet. The pump efficiency η_s was set at 0.8 and the electric efficiency η_{el} at 0.85 (gec-co, 2019).

$$P_{el,P} = (\rho_A \cdot g \cdot \dot{V} \cdot H) \,/\, (\eta_s \cdot \eta_{el}) \tag{1}$$

The heat exchangers (HEX) and evaporators (EVAP) are modeled as ideal counterflow heat exchangers without pressure losses. A constant pinch temperature of 5 K is assumed for the heat transfer. The evaporator is modeled as a serial arrangement of preheater, evaporator and superheater.
A COP-based approach is used to calculate the CLCHP. The COP_{Carnot} indicates the maximum achievable COP of the heat pump and is calculated according to Equation (2). $T_{sink,out}$ corresponds to the outlet temperature of the sink. The temperature lift ΔT_{Lift} is calculated as the difference of $T_{sink,out}$ and the outlet temperature of the source $T_{source,out}$ (Reinholdt *et al.*, 2018). The real efficiency of the heat pump COP_{HP} is estimated by Equation (3) using the exergetic efficiency η_{ex}, which is typically in the range of 0.5 (Klute *et al.*, 2024). The required electrical power consumption of the HP is calculated according to Equation (4), where $\dot{Q}_{sink}$ represents the heat flow rate at the sink side of the HP.

$$COP_{Carnot} = (T_{sink,out}) \,/\, \Delta T_{Lift} \tag{2}$$
$$COP_{HP} = \eta_{ex} \cdot COP_{Carnot} \tag{3}$$
$$P_{el} = \dot{Q}_{sink} \,/\, COP_{HP} \tag{4}$$

The electrical power consumption of the MVR is determined by applying the isentropic efficiency ($\eta_{s,MVR}$ = 0.75) and electric efficiency ($\eta_{el,MVR}$ = 0.95). The maximum possible pressure ratio of a single compressor stage (p_{out}/p_{in}) varies depending on the compressor design and is here assumed to be 2.5 (Klute *et al.*, 2024). Auxiliary pumps are calculated with an overall efficiency of 0.95. Throttles are assumed to be ideally isenthalpic.

3.2 Evaluation criteria

An extended COP definition COP_{PR} is used to evaluate the efficiency of the PRs (Equation 5). In addition to the required energy used for upgrading, all further electric consumers are taken into account.

$$COP_{PR} = \dot{Q}_{sink} \,/\, \sum P_{el,i} \tag{5}$$

For the ecological evaluation, CO_2-Emissions and primary energy demand are used. The CO_2-Emissions Y_{CO_2} are calculated by multiplying the specific CO_2-Emission factor per energy carrier $\bar{e}_{CO_2}$ and the final energy demand E (Equation 6).

$$Y_{CO_2} = \bar{e}_{CO_2} \cdot E \tag{6}$$

The primary energy demand PED is calculated from the total primary energy factor f_t and the corresponding final energy demand E (Equation 7). The total primary energy factor consists of a renewable f_r and a non-renewable component f_{nr}. In this study, both components are considered, as it allows to consider the converting losses of the energy source.

$$PED = f_g \cdot E \tag{7}$$
$$f_t = f_r + f_{nr} \tag{8}$$

The specific factors depend strongly on the origin and production of the energy source and therefore vary for different observation timeframes and locations. Table 2 shows the selected value set for this study which represent possible values for Germany in 2030 and 2045. The green hydrogen is assumed to be produced by proton-exchange-membrane electrolysis (PEMEL) (efficiency 69 % in 2030 and 74 % in 2045 based on (Merten *et al.*, 2020)) from wind energy.

https://doi.org/10.52202/077185-0028

Table 2: Specific CO_2-Emission factor $\bar{e}_{CO_2}$ and total primary energy factor f_t of different energy sources in 2030 and 2045. [1] (BAFA, 2021), [2] (IINAS, 2021), [3] (Notter *et al.*, 2022), [4] (DIN V 18599–1, 2018), [5] own assumptions

	$\bar{e}_{CO_2}$ [t/MWh]		f_t [-]	
	2030	2045	2030	2045
Natural gas	0.201[1]	0.201[1]	1.1[4]	1.1[4]
Electricity (national mix)	0.268[2]	0.032[2]	1.76[2]	1.27[2]
Green hydrogen	0.035[3]	0.035[3]	1.45[5]	1.35[5]
Geothermal	0[5]	0[5]	1[4]	1[4]

4 Results

The performance of a process route is influenced by various internal and external parameters. A sensitivity analysis was carried out to demonstrate the influence of some of these parameters. The injection temperature is one of the most important external parameters, as the heat output can be adjusted by lowering it. However, lowering the injection temperature also leads to a higher temperature lift, which results in a drop in efficiency. Due to technical and regulatory constraints, the injection temperature is usually limited to a lower limit (Welter, 2018). In this study, a minimum value of 60 °C was assumed. In addition, the influence of internal parameters was taken into account. Therefore η_{ex} and $\eta_{s,MVR}$ were varied in the range of 0.4–0.6 and 0.7–0.8.

4.1 Efficiency

Figure 5 shows the results of the two geological sites (G1 and G2). Each data point of the curves represents a specific design for one injection temperature. It is important to note that this is not a representation of part-load behavior. The center line represents the results with default values (η_{ex} = 0.5, $\eta_{s,MVR}$ = 0.75) and is enveloped by an upper (η_{ex} = 0.6, $\eta_{s,MVR}$ = 0.8) and lower (η_{ex} = 0.4, $\eta_{s,MVR}$ = 0.7) curve. In case of low temperature glides of the geothermal water (respectively high injection temperatures), low COP_{PR} are achieved in all cases, as only small amounts of steam are generated but a constant production pump capacity is required. If the injection temperature is lowered, more steam is generated while the pump requires the same amount of energy, resulting in a higher COP_{PR}. After reaching a maximum, the COP drops again due to the decreasing efficiency of the upgrading technology. This transition area from lower to higher COP_{PR} values is strongly influenced by the geological properties of the borehole and is hence location dependent (Klute, 2024).

At location G1, more steam can be generated at the same injection temperature than at location G2, as the temperature level of the source is higher and therefore more usable heat output is available. Since the pumping effort is constant in both cases, higher COP values can be achieved.

Overall, PR3 achieves the highest COP_{PR} at both locations (4.3 at 100 °C and 3.4 at 80 °C). The efficiency advantage of this PR is particularly evident at low reservoir temperatures in combination with high temperature lifts. PR2 achieves COP values between the other two PRs, with overlaps depending on the design parameters. As PR2 combines two HP technologies, additional degrees of freedom arise. By lowering the intermediate pressure (default value 115 °C), the energetic share of the MVR as well as the COP_{HP} would increase, causing the COP_{PR} curves to shift closer to the PR3 values. Increasing the intermediate pressure would shift the curves towards PR1. The serial modeling of the CLCHP at location G1 results in a kink point in the range of 80 °C for PR1 and PR2.

The results show that COP values well above those of electric steam generators can be achieved, which leads to lower energy related operating costs. For the comparison with natural gas or hydrogen boilers, however, other factors like the price ratio of the energy sources (e. g. natural gas to electricity) are relevant as well. Typically, a ratio of around 2 is considered promising. Such a ratio is found, for example, in countries with a high proportion of renewable energies (e. g. Sweden) (Nowak, 2023). For countries with higher price ratios, correspondingly higher COP values must be achieved in order to enable cost-effective operation. If steam is generated via CHP plants instead, the amount of supplied electricity must be taken into account for the assessment as well.

https://doi.org/10.52202/077185-0028

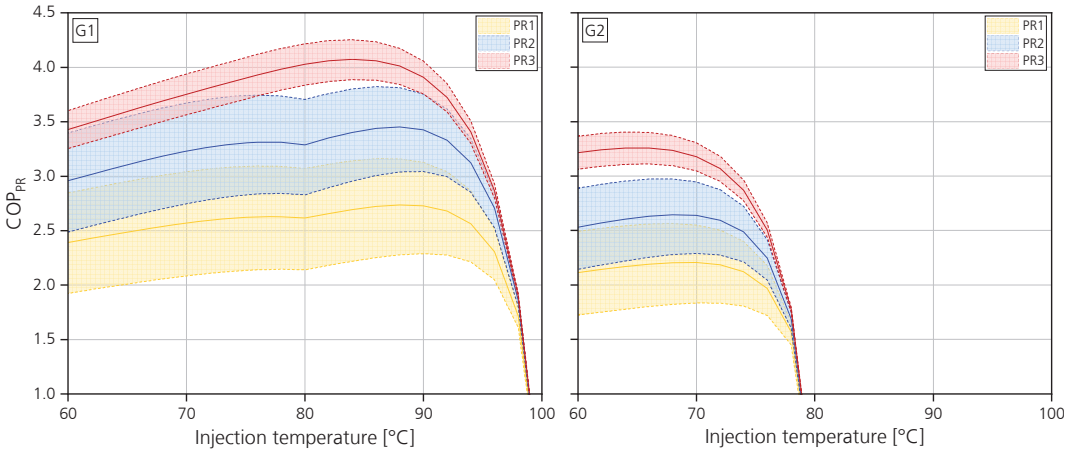

Figure 5: COP_{PR} of the three process routes with variation of the exergetic efficiency η_{ex}, the isentropic efficiency of the mechanical vapor recompression $\eta_{s,MVR}$ and the injection temperature

4.2 Ecological comparison

For ecological assessment, the benchmark technologies (T1, T2 and T3) described in Section 3.1 are considered alongside the three PRs. Figure 6 shows the CO_2-Emissions and PED of the different systems in the years 2030 and 2045. For the comparison, default parametrization of the PRs and a reservoir temperature of 100 °C is used. The steam mass flow rates of the PRs are adjusted by changing the injection temperature. In contrast to the benchmark technologies, the maximum steam output of the PRs is restricted by the minimum injection temperature. The maximum steam output of a PR is closely linked to its efficiency. With lower COP_{PR}values, more energy must be provided for upgrading, resulting in a higher thermal output of the PR.

Despite the remaining share of fossil fuels in the electrical grid (2030), all PRs emit significantly less CO_2 than conventional natural gas boilers (T1). Compared to electric steam boilers (T3), higher COP values are achieved, leading to less emissions. Hydrogen-powered boilers (T2) achieve the lowest emission values when using green hydrogen. However, it should be noted that green hydrogen is not expected to be widely available by 2030 and that its implementation at this time is therefore uncertain. Technology T3 shows the highest value in terms of the PED (2030). T2 achieves only slightly lower values because high conversion losses for suppling the hydrogen. PR1–PR3 require significantly less primary energy than T2 and T3, but slightly more than T1.

In 2045, further integration of renewable energies into the electricity grid and the improvement of production paths are expected to result in lower CO_2-Emissions and PEDs for several technologies. In terms of CO_2-Emissions, T1 and T3 remain unaffected. Despite the higher specific emission factor of the electricity mix compared to green hydrogen, T3 produces fewer emissions than T2 because of its higher efficiency. This correlation is even more evident in the case of the three PRs, which emit the fewest amount of CO_2. The PED of T1 remains at the same level as in 2030. For T2, there is a marginal improvement compared to 2030 thanks to the increased PEMEL efficiency. Due to the decreasing primary energy factor of the electricity mix and the improved conversion efficiency, PED of T3 falls to a level below T2. Geothermal steam generation achieves the lowest PED among the considered technologies.

Comparable results are obtained for the G2 site. In general, there are lower maximum steam outputs (PR1/PR2/PR2, 10/8.6/7.5 t/h) with slightly higher CO_2-Emissions and PED. The discussed effects at location G1 are transferable except for the PED in 2045. In this case, geothermal steam generation results in roughly the same PED as T1. As expected, lower reservoir temperatures therefore lead to lower ecological benefits.

The presented results are strongly dependent on the selected assumptions of the scenarios, which is why they can only be interpreted as a general tendency. Overall, however, the potential of geothermal process steam generation becomes evident, particularly with respect to efficient use of renewable PE. With the technological advancement of (steam-generating) high-temperature heat pumps, this potential will increase even further in the future.

https://doi.org/10.52202/077185-0028

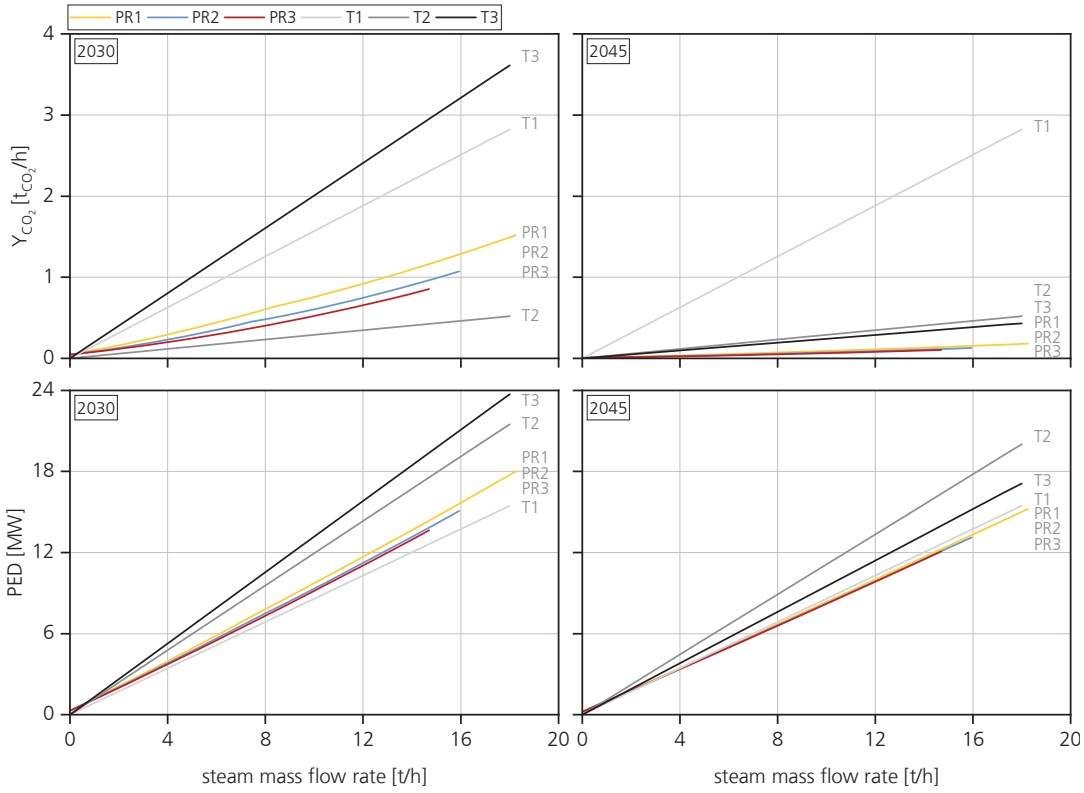

Figure 6: CO_2-Emissions und primary energy demand (PED) for the geothermal process routes (PR1–PR3, reservoir temperature 100 °C) and benchmark technologies (T1–T3)

5 CONCLUSION

Geothermal steam generation has so far only been used at locations with reservoir temperatures above the operating temperatures of the process. In many places, however, the temperature level of the geothermal source is not high enough, leaving the reservoir to be used for other purposes or even unused. By implementing suitable process routes with thermal upgrading, these sources can be made accessible. In this paper, three exemplary PRs were presented and compared with benchmark technologies for steam generation. It was shown that geothermal steam generation can offer energetic and ecologic advantages over electric steam boilers and boilers with natural gas or green hydrogen. In order to increase the transferability of the results, further investigations, such as a variation of the emission factors, optimization of the design parameters (e. g. intermediate pressure of PR2) or cross-variation of the efficiency values (e. g. $\eta_{ex} = 0.6$, $\eta_{s,MVR} = 0.7$) are necessary. In addition, the evaluation should be combined with a financial analysis, as the exploration of the geothermal reservoir is associated with considerable investment cost.

Although geothermal steam generation with thermal upgrading is a new way of using geothermal energy, established technologies to extract the heat from the geothermal water (e. g. in district heating) can be adopted. Due to the novel combination with steam-generating heat pumps, however, detailed studies and first implementation projects are required to investigate the interaction between the subsystems. In addition to the technical issues, further exploration of the underground is essential to ensure that such projects can be implemented on a large scale.

NOMENCLATURE

COP	Coefficient of performance	-
ΔT_{Lift}	Temperature lift	K

https://doi.org/10.52202/077185-0028

$\bar{e}_{CO2}$	Specific CO_2-Emission factor per energy carrier	t_{CO2}/MWh
E	Final energy demand	W
η_{el}	Electric efficiency	-
η_{ex}	Exergetic efficiency	-
η_s	Isentropic efficiency	-
f	primary energy factor	-
g	Standard gravity	m/s^2
H	Delivery head	m
p	Pressure	bar
P	Power	W
$\dot{Q}$	Heat flow rate	W/s
ρ	Density	kg/m^3
T	Temperature at sink outlet	K
$\dot{V}$	Volume flow rate	m^3/s
Y_{CO2}	Specific CO_2-Emission	t_{CO2}/h

Subscript

CLCHP	Closed-Loop Compression Heat Pump
COP	Coefficient of Performance
EVAP	Evaporator
G1, G2	Geothermal Source 1 and 2
HEX	Heat Exchanger
HP	Heat Pump
MVR	Mechanical Vapor Recompression
PED	Primary Energy Demand
PEMEL	Proton-Exchange-Membrane Electrolysis
PR	Process Route
SGHP	Steam Generating Heat Pump
T1, T2, T3	Technology 1, 2 and 3

REFERENCES

Agora Industrie (2022), *Power-2-Heat: Erdgaseinsparung und Klimaschutz in der Industrie,* Version: 1.0.

Agora Industrie, FutureCamp and Wuppertal Institut (2022), "Power-2-Heat: Direkte Elektrifizierung von industrieller Prozesswärme. Rechner für die Abschätzung der Transformationskosten", Modellversion 1.1, 16.09.22, available at: https://www.agora-industrie.de/daten-tools/transformationskostenrechner-power-2-heat (accessed 5 January 2024).

BAFA (2021), *Informationsblatt CO2-Faktoren: Bundesförderung für Energie- und Ressourceneffizienz in der Wirtschaft - Zuschuss*.

Bloomer, A. (Ed.) (2011), *Kawerau direct heat use: historical patterns and recent developments*.

BMWK (2022a), *Zahlen und Fakten: Energiedaten: Nationale und internationale Entwicklungen*.

BMWK (2022b), *Zeitreihen zur Entwicklung der erneuerbaren Energien in Deutschland: unter Verwendung von Daten der Arbeitsgruppe Erneuerbare Energien-Statistik (AGEE-Stat)*.

Bosch (2023), "Planungshandbuch für Dampfkesselanlagen. Professionell planen und effizient auslegen".

Bracke, R. and Huenges, E. (2021), *Roadmap Tiefe Geothermie für Deutschland: Handlungsempfehlungen für Politik, Wirtschaft und Wissenschaft für eine erfolgreiche Wärmewende*, Fraunhofer-Gesellschaft.

Brasser, T., Cannepin, R., Feige, S., Frieling, G., Herber, H.-J., Heinen, C., Strack, C. and Vieten, C. (Eds.) (2014), *GeoSys: Systemanalyse der geothermalen Energieerzeugung ; Teil A Synthesebericht, Teil B Ausführliche Ergebnisdokumentation, GRS*, Vol. 316, GRS, Köln.

Carter, A.C. and Hotson, G.W. (1992), "Industrial use of geothermal energy at the Tasman pulp & paper co. ltd's mill, Kawerau, New Zealand", *Geothermics*, Vol. 21 5–6, pp. 689–700.

DIN V 18599–1 (2018), *DIN V 18599–1: Energetische Bewertung von Gebäuden – Berechnung des Nutz-, End- und Primärenergiebedarfs für Heizung, Kühlung, Lüftung, Trinkwarmwasser und Beleuchtung: Teil 1: Allgemeine Bilanzierungsverfahren, Begriffe, Zonierung und Bewertung der Energieträger*, 91.120.10; 91.140.01 18599–1:2018-09, Beuth Verlag, Berlin.

https://doi.org/10.52202/077185-0028

gec-co (2019), *Wissenschaftlicher Endbericht: Vorbereitung und Begleitung bei der Erstellung eines Erfahrungsberichts gemäß § 97 Erneuerbare-Energien-Gesetz: Teilvorhaben II b): Geothermie*.

HUTTRER, G. (Ed.) (2020), *Geothermal Power Generation in the World 2015-2020 Update Report*.

IINAS (2021), *Kurzstudie: Der nichterneuerbare kumulierte Energieverbrauch und THG-Emissionen des deutschen Strommix im Jahr 2020 sowie Ausblicke auf 2030 und 2050: Bericht für die HEA - Fachgemeinschaft für effiziente Energieanwendung e.V.*, Darmstadt.

Kaltschmitt, M. (2013), *Erneuerbare Energien: Systemtechnik, Wirtschaftlichkeit, Umweltaspekte,* 5., erweiterte Auflage, korrigierter Nachdruck, Springer Vieweg, Berlin.

Klute, S. (2024), *Identifizierung und Bewertung von Verfahrensrouten für die industrielle Prozessdampferzeugung aus Tiefengeothermie: Am Beispiel der Papierindustrie, UMSICHT-Schriftenreihe*, Vol. 106, Laufen.

Klute, S., Budt, M., van Beek, M. and Doetsch, C. (2024), "Steam generating heat pumps – Overview, classification, economics, and basic modeling principles", *Energy Conversion and Management*, Vol. 299, p. 117882.

Lassacher, S., Moser, S. and Lindorfer, J. (2018), *Dokumentation: Industrielle Nutzung von Geothermie*.

Lienau, P.J. and Lunis, B.C. (1991), "Geothermal Direct Use Engineering and Design Guidebook".

Lu, Z., Gong, Y., Yao, Y., Luo, C. and Ma, W. (2019), "Development of a high temperature heat pump system for steam generation using medium-low temperature geothermal water", *Energy Procedia*, Vol. 158 The 10th International Conference on Applied Energy, pp. 6046–6054.

Lund, J.W. (1997), "Milk Pasteurization with Geothermal energy", *GHC Bulletin* Vol. 18, No. 3.

Lund, J.W. (2010), "Direct Utilization of Geothermal Energy", *Energies*, Vol. 3 No. 8, pp. 1443–1471.

Lund, J.W. and Toth, A.N. (2020), "Direct utilization of geothermal energy 2020 worldwide review", *Geothermics*, p. 101915.

Merten, F., Scholz, A., Krüger, C., Heck, S., Girard, Y., Mecke, M. and George, M. (2020), *Bewertung der Vor- und Nachteile von Wasserstoffimporten im Vergleich zur heimischen Erzeugung*.

Notter, B., Cox, B., Hausberger, S., Matzer, C., Weller, K., Dippold, M., Politschnig, N., Lipp, S., Allekotte, M., Knörr, W., Andre, M., Gagnepain, L., Hult, C. and Jerksjö, M. (2022), *HBEFA 4.2 - Documentation of updates*.

Nowak, T. (2023), *Europe´s Heat Pump market: numbers, context, EU policy, European Heat Pump Summit 2023*, Nürnberg, Deutschland.

Pelte, D. (Ed.) (2010), *Die Zukunft unserer Energieversorgung: Eine Analyse aus mathematisch-naturwissenschaftlicher Sicht*, Vieweg+Teubner, Wiesbaden.

Reinholdt, L., Kristofersson, J., Zühlsdorf, B. and et al. (Eds.) (2018), *Heat pump COP, part 1: generalized method for screening of system integration potentials,* Vol. 2, pp. 1097-1104.

Schmitt, B. (2014), *Integration thermischer Solaranlagen zur Bereitstellung von Prozesswärme in Industriebetrieben, Schriftenreihe der Reiner Lemoine-Stiftung*, Shaker, Aachen.

Sigurdsson, F. (1992), "Kísilidjan HF - A unique diatomite plant", *Geothermics*, Vol. 21 5–6, pp. 701–707.

Spoelstra, S. (2019), *Sustainable Steam production in indutry (STEPs): Openbare eindrapportage*, Petten, Niederlande.

Stadtwerke Schwerin, *Geothermie in Schwerin-Lankow - Das Projekt*.

TNO (2020), "TECHNOLOGY FACTSHEET - H2 INDUSTRIAL BOILER", available at: https://energy.nl/wp-content/uploads/h2industrialboiler_28092020_upd-7.pdf.

Ungar, P., Fiaschi, D., Manfrida, G. and Talluri, L. (2023), "Thermodynamic assessment of Geothermal High-Temperature Heat Pumps for Industrial Steam Production".

Vasiljević, R. (2019), "Use of depleted hydrocarbon reservoirs for geothermal energy and its significance in energy transfer toward a low-carbon economy: a paper factory project in Slatina, Croatia", *European Geologist No.* 47.

Walmsley, M., Walmsley, T., Atkins, M. and Neale, J. (2016), "Sustainalbe milk powder production usin enhanced process integration and 100 % renewable energy", *Chemical Engineering Transactions* Vol. 52, pp. 559–564.

Welter, S. (2018), "Technisch-ökonomische Analyse der Energiegewinnung aus Tiefengeothermie in Deutschland", Dissertation, Fakultät Energie-, Verfahrens- und Biotechnik, Universität Stuttgart, 2018.

Zarrouk, S.J. and Purnanto, M.H. (2015), "Geothermal steam-water separators: Design overview", *Geothermics*, Vol. 53, pp. 236–254.

https://doi.org/10.52202/077185-0028